Clinical Cancer Research

The HGF/c-MET Pathway Is a Driver and Biomarker of VEGFR-inhibitor Resistance and Vascular Remodeling in Non–Small Cell Lung Cancer

Tina Cascone[1], Li Xu[1], Heather Y. Lin[2], Wenbin Liu[3], Hai T. Tran[1], Yuan Liu[4], Kathryn Howells[5], Vincent Haddad[5], Emer Hanrahan[1], Monique B. Nilsson[1], Maria A. Cortez[6], Uma Giri[1], Humam Kadara[7,8], Babita Saigal[1], Yun-Yong Park[9], Weiyi Peng[10], Ju-Seog Lee[9], Anderson J. Ryan[5], Juliane M. Jüergensmeier[5], Roy S. Herbst[11], Jing Wang[3], Robert R. Langley[12], Ignacio I. Wistuba[7], Jack J. Lee[2], and John V. Heymach[1,12]

Abstract

Purpose: Resistance to VEGFR inhibitors is a major obstacle in the treatment of non–small cell lung cancer (NSCLC). We investigated the cellular mechanisms mediating resistance of NSCLCs to VEGFR tyrosine kinase inhibitors.

Experimental Design: We generated murine models of human NSCLC and performed targeted inhibition studies with the VEGFR TKIs cediranib and vandetanib. We used species-specific hybridization of microarrays to compare cancer (human) and stromal (mouse) cell transcriptomes of TKI-sensitive and -resistant tumors. We measured tumor microvascular density and vessel tortuosity to characterize the effects of therapy on the tumor vascular bed. Circulating cytokine and angiogenic factor levels in patients enrolled in VEGFR TKI trials were correlated with clinical outcomes.

Results: Murine xenograft models of human lung adenocarcinoma were initially sensitive to VEGFR TKIs, but developed resistance to treatment. Species-specific microarray analysis identified increased expression of stromal-derived hepatocyte growth factor (HGF) as a candidate mediator of TKI resistance and its receptor, c-MET, was activated in cancer cells and tumor-associated stroma. A transient increase in hypoxia-regulated molecules in the initial response phase was followed by adaptive changes resulting in a more tortuous vasculature. Forced HGF expression in cancer cells reduced tumor sensitivity to VEGFR TKIs and produced tumors with tortuous blood vessels. Dual VEGFR/c-MET signaling inhibition delayed the onset of the resistant phenotype and prevented the vascular morphology alterations. In patients with cancer receiving VEGFR TKIs, high pretreatment HGF plasma levels correlated with poorer survival.

Conclusions: HGF/c-MET pathway mediates VEGFR inhibitor resistance and vascular remodeling in NSCLC. *Clin Cancer Res; 23(18); 5489–501. ©2017 AACR.*

Introduction

Most efforts to inhibit angiogenesis as a means to control tumor growth have focused on the VEGF/receptor (VEGF/R) signaling pathway (1–3). Bevacizumab, a recombinant humanized mAb that binds to circulating VEGF and inhibits its function, prolongs both progression-free survival (PFS) and overall survival (OS) of patients with advanced/metastatic non–small cell lung cancer (NSCLC) when it is administered in combination with chemotherapy (4). However, the clinical benefits of anti-VEGF therapies in NSCLC are modest, and many lung and other cancers are either intrinsically refractory to therapy or eventually acquire resistance following continued administration (5–7). Therapeutic resistance

[1]Division of Cancer Medicine and Department of Thoracic and Head and Neck Medical Oncology, The University of Texas MD Anderson Cancer Center, Houston, Texas. [2]Department of Biostatistics, The University of Texas MD Anderson Cancer Center, Houston, Texas. [3]Department of Bioinformatics and Computational Biology, The University of Texas MD Anderson Cancer Center, Houston, Texas. [4]GlaxoSmithKline, Research Triangle Park, North Carolina and Collegeville, Pennsylvania. [5]AstraZeneca, Macclesfield, United Kingdom. [6]Department of Experimental Radiation Oncology, The University of Texas MD Anderson Cancer Center, Houston, Texas. [7]Department of Translational Molecular Pathology, The University of Texas MD Anderson Cancer Center, Houston, Texas. [8]Department of Biochemistry and Molecular Genetics, Faculty of Medicine, American University of Beirut, Beirut, Lebanon. [9]Department of Systems Biology, The University of Texas MD Anderson Cancer Center, Houston, Texas. [10]Department of Melanoma Medical Oncology, The University of Texas MD Anderson Cancer Center, Houston, Texas. [11]Section of Medical Oncology and Department of Developmental Therapeutics, Yale School of Medicine, New Haven, Connecticut. [12]Department of Cancer Biology, The University of Texas MD Anderson Cancer Center, Houston, Texas.

Note: Supplementary data for this article are available at Clinical Cancer Research Online (http://clincancerres.aacrjournals.org/).

Current address for Y. Liu: Pfizer Inc., San Diego, California; current address for E. Hanrahan, St. Vincent's University Hospital, Dublin, Ireland; current address for Y.-Y. Park, ASAN Institute for Life Sciences, ASAN Medical Center, University of Ulsan College of Medicine, Seoul, Korea; current address for A.J. Ryan, Department of Oncology, University of Oxford, Oxford, United Kingdom; and current address for J.M. Jüergensmeier, Gilead Sciences Inc., Foster City, California.

Corresponding Author: John V. Heymach, Departments of Thoracic, Head and Neck Medical Oncology and Cancer Biology, Unit 432, The University of Texas MD Anderson Cancer Center, 1515 Holcombe Blvd, Houston, TX 77030. Phone: 713-792-6363; Fax: 713-792-1220; E-mail: jheymach@mdanderson.org

doi: 10.1158/1078-0432.CCR-16-3216

Translational Relevance

VEGFR inhibitors such as the TKIs vandetanib and cediranib have been shown to improve progression-free survival and response rates, respectively, in patients with NSCLC. However, most lung tumors are either indifferent to these agents or eventually acquire resistance following their continued administration. Here, we used species-specific transcriptomic profiling to identify cancer cell- and stromal-specific alterations associated with resistance to VEGFR TKIs. We identified the HGF/c-MET pathway as a mediator of resistance and vascular remodeling in xenograft models of human NSCLC. Dual VEGFR/c-MET pathway inhibition delayed the onset of the resistant phenotype and prevented resistance-associated sprouting revascularization. This study has direct clinical implications and suggests that combined VEGFR and c-MET blockade may provide superior therapeutic benefit for the treatment of NSCLC. Elevated circulating levels of HGF were associated with a poorer outcome in patients with cancer treated with VEGFR TKIs from three separate clinical trials.

is also a limitation of VEGFR tyrosine kinase inhibitors (TKIs), which target the catalytic domain of VEGFR. Indeed, VEGFR TKIs have not demonstrated an improvement in OS either as monotherapy (8, 9) or in combination with chemotherapy (10–12) in NSCLC patients. Previous investigations led to the identification of several mechanisms that allow tumors to progress on therapies that target the VEGF protein (2, 13, 14). More recent studies have concentrated on an improved understanding of the mechanisms underlying tumor resistance to VEGFR TKIs to develop more effective antiangiogenic therapies.

Accumulating evidence indicates that both cancer cells and stromal cells play a significant role in mediating therapeutic resistance to agents that target the tumor vasculature (15–22). Anti-VEGF therapies are known to reduce oxygen delivery to tumors and the resulting hypoxia stimulates cancer cells and stromal cells to increase their expression of alternative angiogenic proteins (20, 23). Previously, we demonstrated that acquired resistance of experimental murine models of human NSCLC to bevacizumab was due, in large part, to upregulation of EGFR and fibroblast growth factor receptor (FGFR) on tumor-associated stromal cells (13, 24). Antibody blockade of VEGFR1 and VEGFR2 signaling in experimental pancreatic islet tumors also prompted cancer cells and tumor-associated endothelial cells to increase their synthesis and secretion of FGF-related proteins (20). In our studies, we also noted that acquired resistance to bevacizumab was associated with a normalized revascularization phenotype in which tumor blood vessels were covered with pericytes that expressed activated EGFR. Moreover, we found that dual EGFR/VEGF pathway inhibition significantly delayed emergence of the resistant phenotype. However, less information is known regarding the cellular and molecular mechanisms that mediate the resistance of NSCLC to VEGFR TKIs.

To begin to address this issue, herein we examined the efficacy of two VEGFR TKIs, cediranib (CED; AZD2171, AstraZeneca) (25) and vandetanib (ZD6474, Caprelsa, AstraZeneca; ref. 26), in murine models of human NSCLC. We applied species-specific gene expression profiling analysis to NSCLC tumors that were sensitive and resistant to TKIs to identify the origin of candidate signaling pathways that may be responsible for the drug-tolerant phenotype. We validated the findings in our models and then assessed their contribution to the human disease in patients with NSCLC and metastatic renal cell carcinoma (mRCC) that were enrolled in clinical trials evaluating VEGFR TKIs.

Materials and Methods

In vivo studies

Male athymic nude mice (NCI-nu) were purchased from the National Cancer Institute (NCI). The mice were maintained in facilities approved by the American Association for Accreditation of Laboratory Care (AAALAC) and according to institutional guidelines. H1975 and A549 NSCLC cells (2×10^6 cells) were injected subcutaneously into 6-week-old male mice, and when tumor size reached approximately 270 mm^3, animals were randomized to the following treatment groups: vehicle [PBS] orally daily; vandetanib 50 mg/kg orally daily; or cediranib 6 mg/kg orally daily. Parallel short-term treatment studies (14 days) were conducted in H1975 tumors when the tumor volume average reached approximately 350 mm^3. The tumor volume average in treated versus control group calculated at the final tumor evaluation was used as index to assess the antitumor activity of cediranib and vandetanib. Tumors were considered resistant when their volume tripled when compared to pretreatment volume, and PFS was defined as the time from treatment initiation until the tumor volume tripled. Animals were euthanized when tumor burden was reached (progression) or for morbidity, according to animal protocol guidelines. We defined the progression vehicle control as the vehicle (PBS)-treated animals that are the control group for the long-term treatment experiment and sensitive vehicle control as the vehicle treated animals for the short-term experiment (14 days). Tumors were excised and processed for immunostaining studies, and a portion of each tumor was also snap-frozen in liquid nitrogen. Hematoxylin and eosin staining was used to confirm the presence of tumor.

Orthotopic lung tumors were produced by implanting H441 lung adenocarcinoma cells (1×10^6) in 50-μL HBSS containing 50-μg growth factor–reduced Matrigel (BD Biosciences) into the left lungs of 6-week-old nude mice, as described previously (13, 27). We euthanized eight mice 3 weeks after implanting the cancer cells to determine the kinetics of tumor growth. Animals were treated with either vehicle (PBS) 100 μL orally daily or vandetanib 50 mg/kg orally daily and euthanized when moribund.

For HGF-stable transfection *in vivo* studies, HCC827-vector, -HGF.20, H1975-vector, or -HGF.24 cancer cells (2×10^6 cells) were implanted subcutaneously into 6-week-old male mice. Treatment was initiated when tumor volumes reached ~300 mm^3. Cabozantinib (XL184) 30 mg/kg and bevacizumab 10 mg/kg were administered orally daily and into the peritoneal space (intraperitoneal) twice a week, respectively. Control mice were treated with PBS administered orally daily and intraperitoneally twice weekly. PFS was defined as time from treatment initiation to tumor volume doubling.

Gene expression profiling: sample preparation and analysis

Total RNA was extracted from snap-frozen tissues using *mir*Vana miRNA Isolation Kit (Ambion), according to manufacturer's protocol. Biotin-labeled cRNA samples for hybridization

were prepared using the Illumina Total Prep RNA amplification kit (Ambion). One microgram of total RNA was used for the synthesis of cDNA, followed by amplification and biotin labeling. Next, 1.5 μg of biotinylated cRNAs was hybridized to human WG-6 v3.0 and mouse WG-6 v2.0 Expression BeadChips (Illumina) for analysis of tumor (human) and stromal (mouse) transcriptomes, respectively. Previous testing of the human and murine microarray platforms determined that they provide sufficient specificity to discriminate expression of mouse and human genes when mRNA from both species is mixed together and that they maintain the necessary sensitivity to detect the expression of species-specific genes even when they only represent 10% of mRNA in the mixture (28). Signals were developed by Amersham fluorolink streptavidin-Cy3 (GE Health Care Bio-Sciences). Gene expression data were collected using the Illumina bead array reader confocal scanner (BeadStation 500GXDW). Quantile normalization was performed on the average signal intensity values of the probes. The normalized expression data were logarithm transformed (base 2) for further analysis. To reveal significant genes within all treatment groups, a linear regression model was fitted and specific contrasts were tested for significance for each probe using the R package *limma* (29). The comparisons made in our study were CED-resistant versus CED-sensitive tumors ("CED prog. vs. CED sens.") and vandetanib-resistant versus vandetanib-sensitive tumors ("VAN prog. vs. VAN sens.") for both human and mouse samples. To determine significance, a beta-uniform model was applied to adjust for multiple comparisons (30). We chose a false discovery rate (FDR) of 0.1 to identify any genes that were significantly modulated. Comparisons between specific treatment groups were performed using the same FDR, with an additional fold change cutoff (>1.5-fold). Finally, we applied the method to specific gene lists consisting of genes known to be associated with angiogenesis, hypoxia, and lymphangiogenesis (31). The gene expression data are deposited in GEO-NCBI database under the accession number GSE64472.

Phase II and phase III study designs and plasma analysis

In this retrospective analysis, we obtained data from three multicenter clinical trials. The first study was a phase II randomized clinical study evaluating vandetanib alone, carboplatin and paclitaxel, or the combination of vandetanib plus carboplatin and paclitaxel in patients with advanced/metastatic NSCLC in the first-line setting (12). The second study was a randomized study evaluating vandetanib or erlotinib in patients with refractory NSCLC (8). The third study consisted of an open-label phase II trial evaluating pazopanib in patients with metastatic renal cell carcinoma (RCC; refs. 32, 33). Details and results of all three trials have been published previously. Clinical protocols and informed consent documents were approved by participating local institutional review boards and the trials were undertaken in accordance with the International Conference on Harmonisation Guidelines for Good Clinical Practice, and the amended Declaration of Helsinki. All patients provided written informed consent before study entry. Blood samples were collected prior to treatment, processed, stored and analyzed for HGF concentration as detailed (see Supplementary Materials and Methods for details).

Biostatistics and standard methods

Statistical and bioinformatics methods, reagents, cancer cells and cell culture conditions, quantitative real-time PCR, immunostaining, HGF stable transfection and vascular morphology analysis are described in Supplementary Materials and Methods.

Results

NSCLC xenografts acquire resistance to VEGFR TKIs

We evaluated the efficacy of cediranib and vandetanib in NSCLC xenograft models. H1975 or A549 NSCLC tumor-bearing animals were treated with vehicle, cediranib, or vandetanib until mice were euthanized due to tumor burden (progression). The individual tumor growth curves of H1975 and A549 xenografts that received vehicle and cediranib are shown in Supplementary Fig. S1A and S1B, respectively. The individual tumor growth curves of vehicle and vandetanib treatment are shown in Supplementary Fig. S1A (H1975) and Supplementary Fig. S1B (A549) and in our prior published studies (13). After initial tumor shrinkage, three H1975 xenografts and two A549 xenografts acquired resistance to CED long-term treatment. In H1975 xenografts, two animals acquired resistance to vandetanib after 148 days of treatment; in A549 xenografts, one animal acquired resistance to vandetanib after 102 days of treatment (13). The gray arrows indicate the resistant xenograft-bearing animals and when they were euthanized due to tumor burden. We obtained tumor tissues from xenograft-bearing animals that were responding to therapy by treating H1975 tumors with cediranib or vandetanib for a period of 14 days (short-term treatment). Animals were euthanized after 2 weeks of treatment or earlier, if necessary, due to tumor burden or morbidity. H1975 xenografts treated with cediranib or vandetanib were smaller than controls at 14 days (cediranib induced an 84% tumor growth reduction vs. vehicle; vandetanib induced a 69% tumor growth reduction vs. vehicle, Supplementary Fig. S1C). The control group has been previously shown (13). These findings suggest that the response of H1975 and A549 NSCLC xenografts model the acquired resistance that takes place in the clinic in which tumors are initially sensitive to VEGFR inhibition, but develop resistance following prolonged treatment.

Angiogenic genes are upregulated in stromal cell and cancer cell compartments in VEGFR TKI-resistant NSCLC xenografts

To identify candidate angiogenic factors that may mediate acquired resistance to VEGFR TKIs, we performed species-specific (human: cancer cells; mouse: tumor stroma) gene expression profiling on cediranib- and vandetanib-sensitive H1975 tumors (short-term treatment) and to tumors that progressed after prolonged treatment. This analysis revealed that seven stromal (mouse) angiogenic genes were significantly modulated in both vandetanib- and cediranib-resistant tumors when compared with vandetanib- and cediranib-sensitive tumors (Fig. 1A). The heatmaps depicting the expression of these seven commonly modulated stromal angiogenic genes are shown in Fig. 1B and C. In tumors that progressed while receiving vandetanib, stromal *Rps7*, *Eng*, *Nos3*, *Hgf*, and *Cxcl1* genes were upregulated, and *Rpl37* and *Npy* genes were downregulated (Fig. 1B; Supplementary Table S1). In tumors that progressed while receiving cediranib, stromal *Hgf*, *Cxcl1*, *Nos3*, and *Eng* genes were upregulated, whereas *Rps7*, *Npy*, and *Rpl37* genes were downregulated (Fig. 1C; Supplementary Table S2).

Fourteen cancer cell (human) angiogenic genes were differentially expressed and shared by tumors that progressed while receiving vandetanib or cediranib treatments compared with

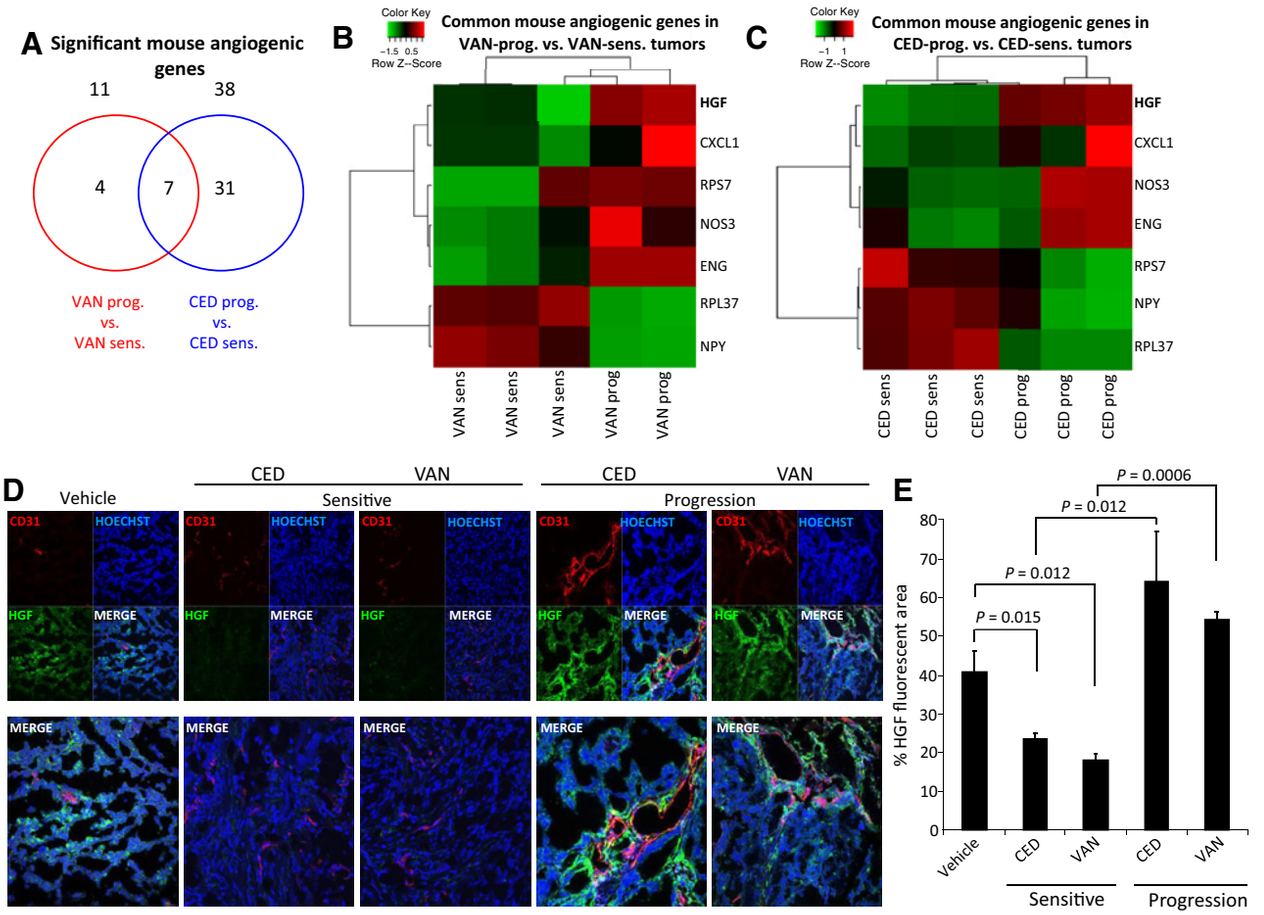

Figure 1.

VEGFR TKI resistance is associated with increased stromal HGF in H1975 xenografts. **A,** Venn diagram of stromal (mouse) angiogenic genes significantly modulated in H1975 tumors with acquired resistance (prog) to vandetanib (VAN; red) or cediranib (CED, blue) versus vandetanib- or cediranib-sensitive tumors (14 days of treatment). **B** and **C,** Heatmaps showing seven common stromal angiogenic genes significantly modulated in both H1975 vandetanib –prog. vs. –sens. tumors (**B**) and H1975 cediranib–prog. vs. –sens. tumors (**C**). When there are more than one significant probe for a gene, the mean of the expression values across the probes were used for the heatmaps in **B** and **C**. **D,** Representative immunofluorescent staining for CD31 (red), HGF (green), and DAPI (blue) in confocal microscopy (×200) of H1975 tumors treated with vehicle, cediranib, or vandetanib for 14 days (sensitive) or until progression; $n = 2$–4 samples/group. **E,** Quantification of HGF^+ staining (% HGF-fluorescent area: green/blue fluorescence) in H1975 tumors (≥5 microscopic fields/sample) treated with vehicle, cediranib, or vandetanib. Data graphed as percentage ± SEM. *P* values are from *t* test. In **D** and **E**, vehicle-treated samples were pooled for this analysis from both vehicle short-term and long-term groups.

vandetanib- and cediranib-sensitive tumors (Supplementary Fig. S2A–S2C; Supplementary Tables S3 and S4). This group of shared angiogenic genes included *IL6* and *HIF3A*. *HIF3A* encodes an adaptor protein in TGFβ signaling modulation of angiogenesis and cell-cycle progression, which were upregulated in both sets of resistant tumors. *CASP1*, an enzyme and member of the caspase family that plays a role in apoptosis, was downregulated in vandetanib- and cediranib-resistant tumors.

HGF/c-MET axis is overexpressed and activated in NSCLC murine models of VEGFR TKI resistance

Stromal *Hgf* gene expression was upregulated in both vandetanib- and cediranib-resistant tumors and other investigators have reported alterations in HGF signaling in tumors resistant to antiangiogenic agents (34). Therefore, we performed additional experiments to determine the contribution of HGF to VEGFR resistance in our models. First, we validated HGF and c-MET at the protein level in H1975 tumors by immunostaining. The HGF staining area was significantly smaller in cediranib- or vandetanib-sensitive tumors compared with control tumors; however, HGF expression increased dramatically in tumors that acquired resistance to cediranib and vandetanib treatments (Fig. 1D and E). Total c-MET expression levels were significantly increased in resistant tumors when compared with cediranib- and vandetanib-sensitive tumors (Fig. 2A and B). We observed higher expression of the activated form of c-MET (p-MET) in vandetanib-resistant versus vandetanib-sensitive tumors in both cancer cell and stromal compartments (Supplementary Fig. S3). We also noted that p-MET expression localized to tumor-associated endothelium of H1975 vandetanib-resistant tumors, but not to endothelial cells of vandetanib-sensitive and control tumors (Fig. 2C). These findings indicate that HGF/c-MET pathway is upregulated in both cancer cells and stromal cells of VEGFR TKI–resistant tumors.

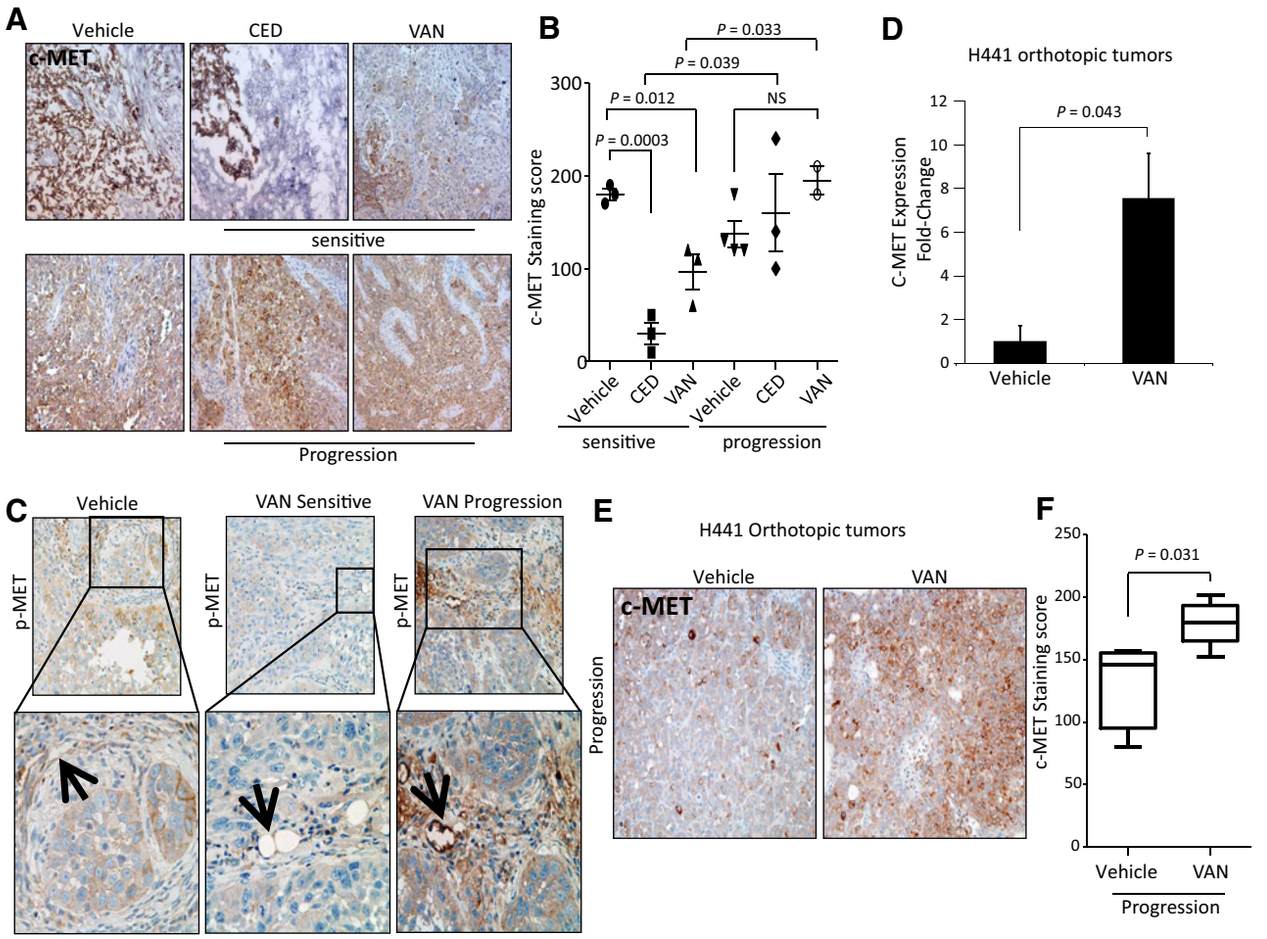

Figure 2.

c-MET is overexpressed and activated in VEGFR TKI–resistant NSCLC murine models. **A,** Representative IHC staining (×200) and **B,** Quantification of total c-MET in H1975 tumors treated with vehicle, cediranib, or vandetanib. Data graphed as mean score (overall intensity) ± SEM. **C,** Representative IHC images (×200 top; ×400 bottom) for phosphorylated c-MET (p-MET) in H1975 tumors treated with vehicle ($n = 3$), vandetanib for 14 days ($n = 3$), or until progression ($n = 2$). At least three photomicrographs were collected per sample. Data graphed as mean score ± SEM. *P* values are from *t* test. The black arrows indicate the localization of positive p-MET staining on tumor-associated endothelium. **D,** Quantitative reverse-transcriptase PCR shows human c-*MET* mRNA expression levels in H441 orthotopic tumors treated with vehicle or vandetanib until progression ($n = 4$/group). Data are normalized relative to mRNA levels in vehicle-treated samples and graphed as mRNA relative levels ± SEM. *P* values are from *t* test. **E,** Representative IHC staining (×100) for c-MET in H441 orthotopic tumors treated with vehicle or vandetanib until progression (≥5 photomicrographs/sample, $n = 4$–5/group). **F,** Quantification of the c-MET immunostaining in H441 tumors treated with vehicle or vandetanib until progression (≥3 core fields/sample quantified). Data shown as mean score ± SEM. *P* values are from *t* test.

Given that the organ microenvironment plays a significant role in determining a cancer cell's responsiveness to treatment (5), we examined the contribution of c-MET signaling to the VEGFR TKI–resistant phenotype in an orthotopic model of lung adenocarcinoma (13). We analyzed H441 orthotopic tumors that were treated with either vehicle or vandetanib until progression and found that cancer cell (human) *c-MET* mRNA expression levels, as well as total c-MET staining area, significantly increased in vandetanib-resistant tumors compared with controls (Fig. 2D–F).

VEGFR inhibitor resistance is HGF-dependent

To determine whether HGF/c-MET signaling is sufficient to confer resistance of NSCLC to the VEGFR TKIs, we transfected HCC827 and H1975 human lung adenocarcinoma cells (35) with the human *HGF* gene (Supplementary Fig. S4A and S4B). The resulting HCC827-vector, H1975-vector, and HGF-overexpressing (HCC827-HGF.20 and H1975-HGF.24) cells were implanted into nude mice and once tumors were established, the animals were treated with VEGF/R inhibitors. In HCC827-vector and HGF.20 xenografts, CED decreased tumor growth after 28 days of treatment compared with vehicle (CED vs. vehicle vector $P = 0.057$; CED vs. vehicle -HGF.20 $P = 0.015$); however, reduced sensitivity to therapy was noted in tumors overexpressing HGF and treated with both CED and bevacizumab compared with vector controls receiving the same treatments (CED HGF.20 vs. CED vector control; $P = 0.023$; bevacizumab HGF.20 vs. bevacizumab vector control $P = 0.035$; Fig. 3A). These results indicate that high HGF expression may render tumors less sensitive to VEGF/R pathway inhibitors.

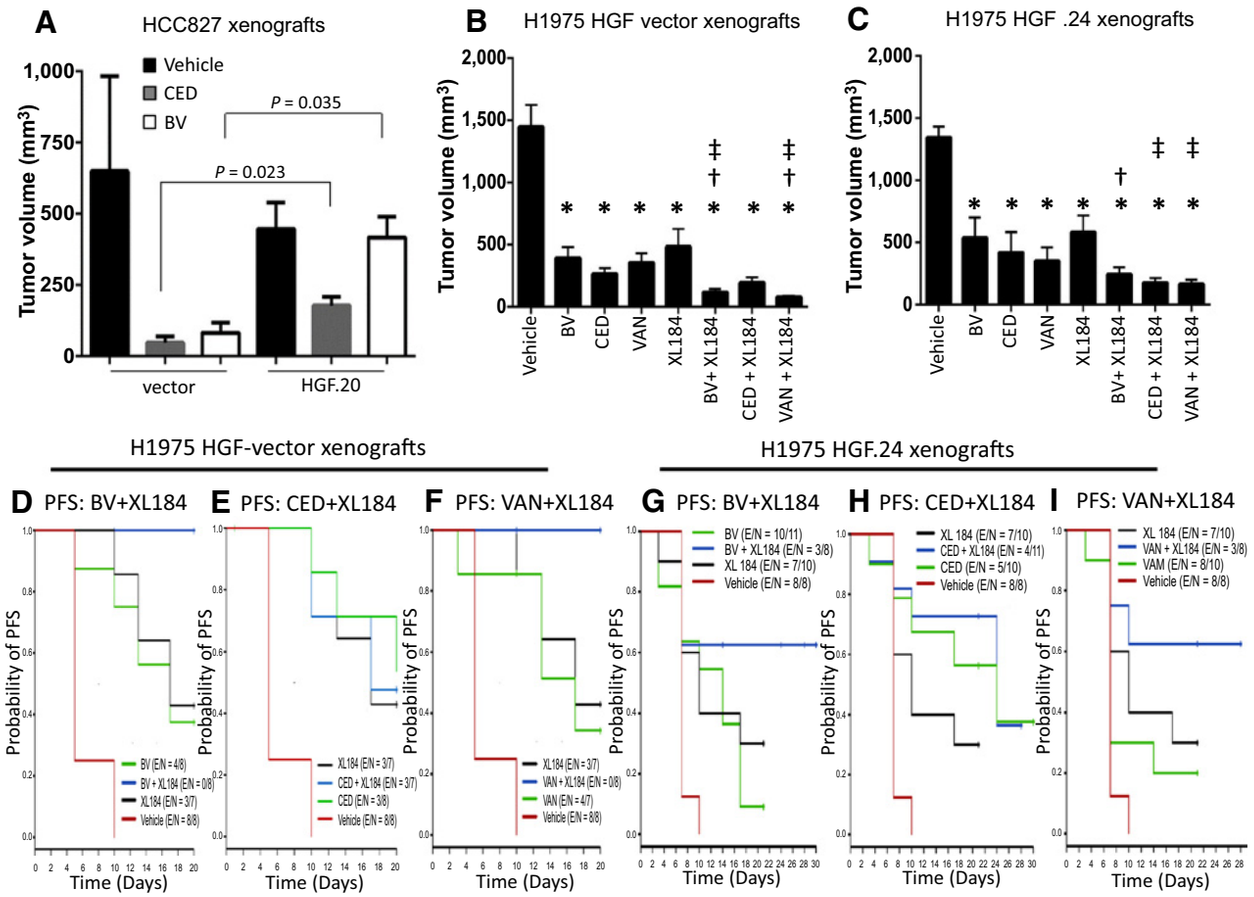

Figure 3.

Ectopic HGF overexpression reduces sensitivity of NSCLC xenografts to VEGF/R inhibitors and dual VEGFR2/c-MET blockade prolongs PFS of NSCLC murine models. **A,** Mean tumor volume differences (±SEM) following bevacizumab (BV) and cediranib 28-day treatment in HCC827-vector and -HGF.20 xenografts (at 28-day point: vector xenografts $n = 3$–4/group; HGF.20 xenografts: $n = 5$/group). P is from Mann–Whitney test. **B** and **C,** Tumor growth inhibition following 17 days of treatment with bevacizumab, cediranib (CED), vandetanib (VAN), or XL184 alone or in combination in H1975-vector ($n = 4$–7/group; **B**) and -HGF.24 xenografts ($n = 7$–10/group; **C**). Data graphed as mean tumor volume at day 17 of treatment ± SEM. *, $P < 0.05$ in the indicated treatment group versus vehicle; †, $P \leq 0.05$ in bevacizumab + XL184 versus bevacizumab and in vandetanib + XL184 versus vandetanib in vectors, and in bevacizumab + XL184 versus bevacizumab in HGF.24 xenografts; ‡, $P < 0.05$ in bevacizumab + XL184 versus XL184, cediranib + XL184 versus XL184 and vandetanib + XL184 versus XL184. P values are from Mann–Whitney test. **D–I,** Kaplan–Meier curves show probability of PFS (time to tumor doubling) of mice bearing H1975 vector control tumors (**D–F**) or H1975-HGF.24–overexpressing tumors (**G–I**) treated with vehicle, bevacizumab, cediranib (CED), vandetanib (VAN), and cabozantinib (XL184) or combination treatments. H1975 vector xenografts: overall $P < 0.0001$; bevacizumab + XL184 versus bevacizumab, $P = 0.015$ (**D**); bevacizumab + XL184 versus XL184, $P = 0.024$ (**D**); cediranib + XL184 versus cediranib, $P = 0.73$ (**E**); cediranib + XL184 versus XL184, $P = 0.95$ (**E**); vandetanib + XL184 versus vandetanib, $P = 0.017$ (**F**); vandetanib + XL184 versus XL184, $P = 0.033$ (**F**). H1975 HGF.24 xenografts: overall $P = 0.004$; bevacizumab + XL184 versus bevacizumab, $P = 0.062$ (**G**); bevacizumab + XL184 versus XL184, $P = 0.23$ (**G**); cediranib + XL184 versus CED $P = 0.64$ (**H**); CED + XL184 versus XL184 $P = 0.074$ (**H**); vandetanib + XL184 versus vandetanib $P = 0.064$ (**I**); vandetanib + XL184 versus XL184, $P = 0.19$ (**I**). The P values are from log-rank test.

Combined VEGFR2/c-MET targeting inhibits tumor growth and prolongs survival in murine models of NSCLC

To determine the therapeutic efficacy of combined inhibition of VEGFR2 and c-MET signaling, we treated mice bearing established H1975-vector and -HGF.24 tumors with bevacizumab, cediranib, or vandetanib alone or in combination with cabozantinib (XL184), a c-MET and VEGFR2 TKI (36). H1975-vector xenografts were sensitive to bevacizumab, cediranib, vandetanib, and XL184 treatments and the combinations bevacizumab + XL184 or vandetanib + XL184 had a more profound antitumor effect than each agent monotherapy (Fig. 3B). Combination treatment with bevacizumab or vandetanib plus XL184 also significantly prolonged the median PFS compared with each agent alone (Fig. 3D and F). H1975-HGF.24 tumors were relatively less sensitive to VEGFR inhibitors than vector controls (Fig. 3C). XL184 combined with bevacizumab, cediranib, or vandetanib inhibited tumor growth of HGF.24 xenografts more than any single agent (Fig. 3C). Combined treatments resulted in a trend to significantly longer PFS than mice receiving bevacizumab, vandetanib, or XL184 alone (Fig. 3G and I). Combination with cediranib plus XL184 was slightly more effective compared with each single agent in HGF-overexpressing tumors (Fig. 3H) and compared with cediranib plus XL184 in HGF-vector tumors (Fig. 3E). These findings suggest

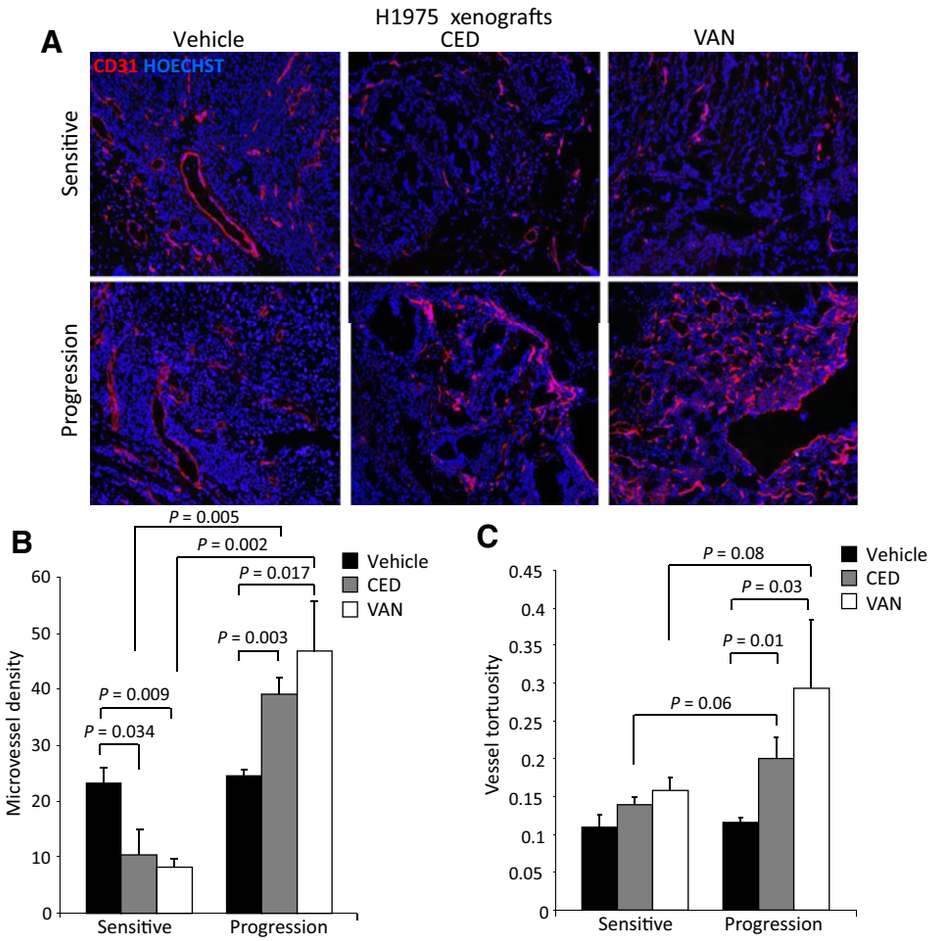

Figure 4.
Tumor vasculature morphology is altered in NSCLC xenograft models that are sensitive or resistant to VEGFR TKIs. **A,** Representative photomicrographs (×100) of CD31+ tumor vessels (red) in H1975 xenografts treated with vehicle, cediranib (CED), or vandetanib (VAN) for 14 days or until progression (≥5 microscopic fields/sample). **B** and **C,** Quantification of MVD (**B**) and vessel tortuosity (**C**) based on CD31-stained tumor sections (≥5 microscopic fields/sample at ×200 for MVD and ≥5 microphotographs/sample at ×100 for vessel tortuosity) in H1975 xenografts treated with vehicle, cediranib (CED), or vandetanib (VAN) for 14 days or until progression ($n = 2$–4/group). Data shown as mean ± SEM. *P* values are from a *t* test.

that dual VEGFR2/c-MET axis blockade delays tumor growth of NSCLCs that overexpress HGF.

HGF overexpression increases vessel tortuosity and combined VEGFR2/c-MET targeting normalizes the tumor-associated vasculature in NSCLC xenografts

To determine the effects of therapy on the tumor vascular bed, we measured the microvascular density (MVD) of VEGFR TKI–treated H1975 tumors and determined that MVD was significantly reduced in cediranib- and vandetanib-sensitive tumors (Fig. 4A and B, left). However, the MVD of resistant tumors (progression) actually increased compared with vehicle-treated and VEGFR TKI-sensitive tumors (Fig. 4B, right) and the blood vessels perfusing the resistant tumors were more tortuous and disorganized (Fig. 4C).

Next, we determined the effect of HGF on tumor vessels by comparing the tumor vasculature patterns of H1975-HGF.24 tumors and vector controls. There were no significant differences in the MVD between vehicle-treated H1975-vector tumors and HGF.24 tumors (Fig. 5A and B). However, we noted that the vessel tortuosity was significantly increased in vehicle-treated HGF-overexpressing tumors ($P < 0.05$; Fig. 5C). In H1975-vector xenografts, the administration of cediranib, vandetanib, XL184, and vandetanib + XL184 treatments significantly decreased MVD compared with vehicle ($P < 0.05$; Fig. 5D, left), whereas in vehicle-treated HGF.24 xenografts, no MVD changes were observed. Both cediranib and vandetanib treatments induced revascularization in HGF-overexpressing tumors (Fig. 5D, right). Dual VEGFR2/c-MET inhibition with XL184 or cediranib + XL184 reduced the MVD in HGF.24 xenografts compared with cediranib or vandetanib alone ($P < 0.05$, Fig. 5D). Vessels supplying vehicle-treated HGF.24 xenografts were more tortuous and disorganized than the blood vessels of vehicle-treated vector xenografts ($P = 0.01$; Fig. 5C and E), and c-MET blockade alone or in combination with VEGFR inhibition significantly reduced vessel tortuosity ($P < 0.05$; Fig. 5E) of HGF-overexpressing tumors.

Intratumoral hypoxia increases in NSCLC tumors following VEGFR inhibition

The studies above indicate that administration of VEGFR TKIs significantly reduces the vascular surface area of H1975 tumors. To determine any functional consequences of the reduced MVD, we quantified levels of the hypoxic biomarker carbonic anhydrase IX (CAIX) in experimental H1975 tumors. We noted that CAIX levels significantly increased in H1975 tumors that were sensitive to vandetanib when compared with vehicle-treated tumors ($P = 0.02$; Supplementary Fig. S5A and S5B) and remained elevated once tumors acquired resistance to vandetanib treatment.

Collectively, these data suggest that short-term administration of VEGFR TKIs inhibits tumor angiogenesis in VEGFR TKI-sensitive tumors. The reduction in tumor microvascular surface area then leads to declining oxygen tensions in the tumor

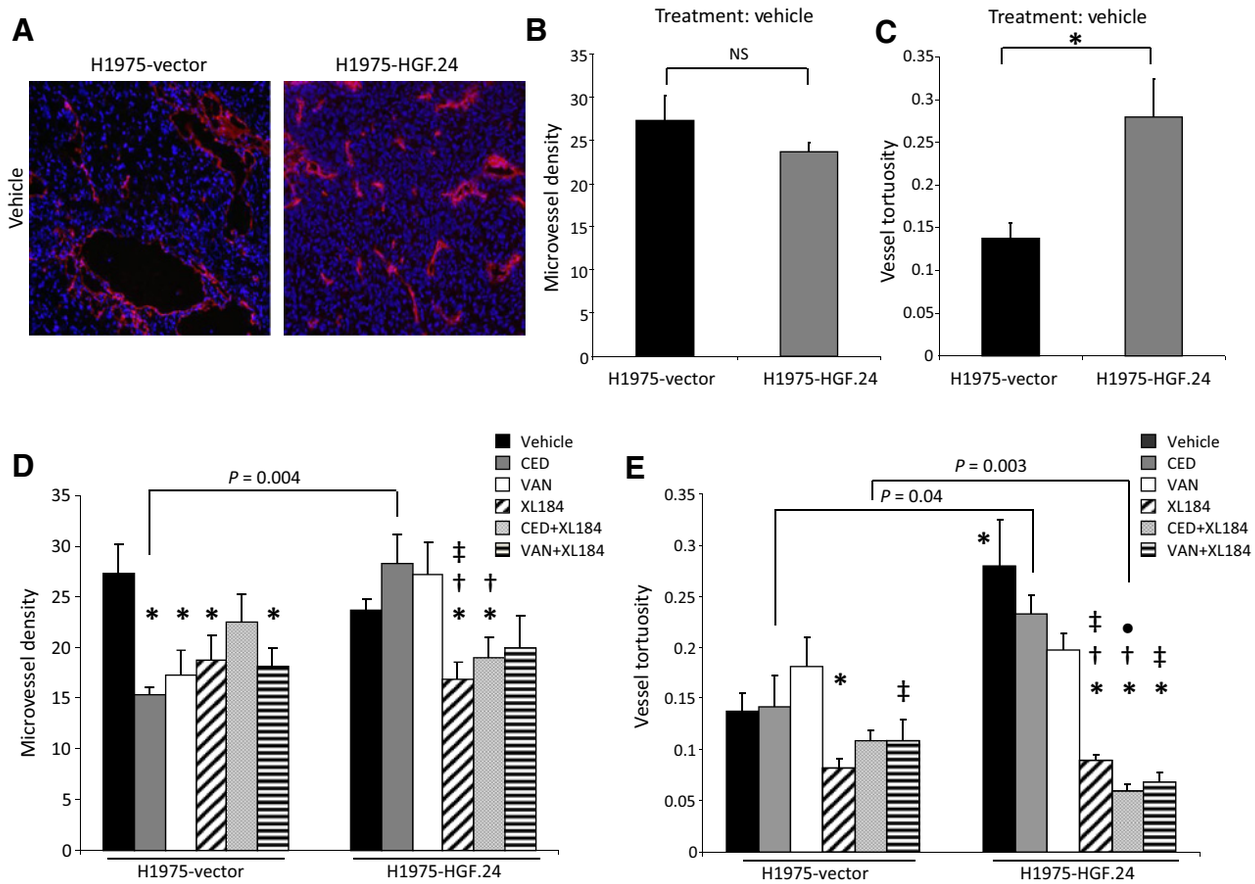

Figure 5.

Altered patterns of tumor vasculature are HGF-dependent in NSCLC models of VEGFR TKI resistance. **A,** Representative IF staining (×100) of $CD31^+$ (red) and nuclei (blue), **B,** MVD and **C,** vessel tortuosity quantification in H1975-vector and -HGF.24 xenografts treated with vehicle for 17 days, which was the time point by when all the animals in vehicle group had been euthanized. **D,** MVD and **E,** vessel tortuosity quantification in H1975-vector and -HGF.24 xenografts treated with vehicle, cediranib, vandetanib, or XL184 alone or in combination. In all panels, data shown as mean ± SEM. *P* values are from *t* test. In HGF-vectors: *, $P < 0.05$ in indicated group versus vehicle; †, $P < 0.05$ in indicated group versus cediranib; ‡, $P < 0.05$ in indicated group versus vandetanib. In HGF.24 xenografts: *, $P < 0.05$ in vehicle versus HGF-vector vehicle group, and in indicated group versus vehicle; †, $P < 0.05$ in indicated group versus cediranib; ‡, $P < 0.05$ in indicated group versus vandetanib. •, $P < 0.05$ in indicated group versus XL184 ($n = 6$–10/group).

microenvironment resulting in upregulation and activation of proangiogenic pathways, such as the HGF/c-MET axis, that restore tumor progression.

High baseline circulating HGF levels are associated with poor outcomes in patients with NSCLC and metastatic renal cell carcinoma (mRCC)

Next, we validated our preclinical findings in samples from patients with NSCLC and RCC enrolled in clinical trials evaluating VEGFR TKIs. We analyzed levels of circulating HGF in patients from three clinical studies and compared PFS among groups (8, 12, 32). The first study was a phase II randomized study of patients with advanced NSCLC treated with vandetanib alone, vandetanib plus carboplatin and paclitaxel (VCP), or carboplatin and paclitaxel alone (control group; ref. 12). After controlling for sex and smoking status in all groups, we determined that elevated plasma HGF was predictive of reduced PFS benefit for vandetanib versus carboplatin and paclitaxel ($P_{interaction} = 0.036$; Fig. 6A and B). Supplementary Table S5 shows median PFS by treatment arm for patients with low and high baseline plasma HGF levels. Among patients who received vandetanib, low baseline plasma HGF levels were associated with superior PFS versus high baseline levels [HR = 1.437 per twofold increase; 95% confidence interval (CI) = 1.038–1.988; $P = 0.029$). However, among patients treated with carboplatin and paclitaxel alone, those with low baseline plasma HGF had equivalent or inferior PFS compared with patients with high plasma HGF levels (Fig. 6A and B).

The second study was a phase III trial evaluating the efficacy of vandetanib versus erlotinib in unselected patients with advanced NSCLC who had progressed after receiving one to two prior chemotherapy regimens (8). We performed an exploratory analysis for 623 patients treated with vandetanib (300 mg orally daily) and 617 patients treated with erlotinib (E; 150 mg orally daily) by HGF status; patients were defined as positive if their pretreatment (baseline) HGF levels were greater than or equal to the median value at baseline, negative if their pretreatment HGF levels did not meet the criteria for positive, and unknown if they did not have a

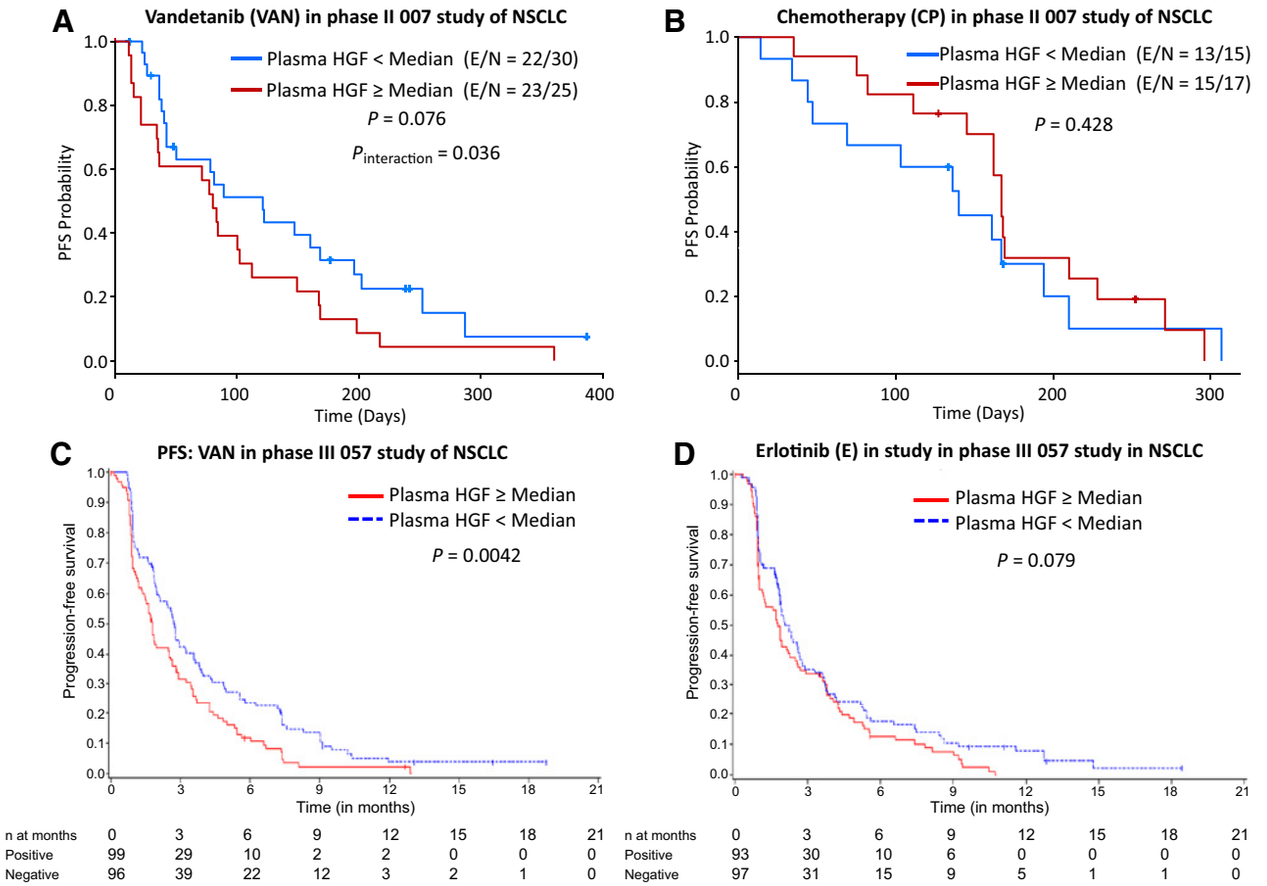

n at months	0	3	6	9	12	15	18	21
Positive	99	29	10	2	2	0	0	0
Negative	96	39	22	12	3	2	1	0

n at months	0	3	6	9	12	15	18	21
Positive	93	30	10	6	0	0	0	0
Negative	97	31	15	9	5	1	1	0

Figure 6.

Plasma HGF levels predict poor outcome in patients with NSCLC treated with VEGFR TKIs. **A** and **B,** Kaplan–Meier (KM) plots showing PFS probability according to baseline plasma HGF levels in patients with NSCLC treated with carboplatin and paclitaxel (CP) or vandetanib (VAN). The $P_{interaction}$ compares the risk of progression (HR) in patients with high plasma HGF levels between carboplatin and paclitaxel and vandetanib arms. **C** and **D,** KM plots showing PFS probability according to baseline plasma HGF levels in patients with NSCLC treated with vandetanib (VAN) or E in the phase III of NSCLC.; E, erlotinib. *P* is from log-rank test.

baseline HGF value. Patients with positive HGF levels experienced slightly poorer outcomes in response to vandetanib versus erlotinib treatment [median PFS: 7.7 vs. 7.6 weeks, respectively; events/number of patients: 93/99 vs. 88/93, HR 1.1 (95% CI, 0.82–1.49; Supplementary Table S6)]. However, positive patients receiving vandetanib had a significantly poorer PFS compared with negative patients treated with vandetanib (median PFS: 7.7 vs. 11.7 weeks, respectively; events/number of patients: 93/99 vs. 88/96, $P = 0.0042$), as shown in Fig. 6C and Supplementary Table S6. No significant differences in PFS were noted in patients receiving erlotinib by HGF status ($P = 0.079$; Fig. 6D). These findings confirm the predictive role of HGF as biomarker of resistance to treatment with vandetanib in NSCLC.

We then questioned whether our findings could be applied to patients treated with VEGFR inhibitors in other malignancies. In a separate open-label, single-arm phase II study (VEG102616, NTC00244764), pazopanib (Votrient, GlaxoSmithKline), a multi-VEGFR TKI, had significant clinical activity in mRCC patients, demonstrating an overall RR of 35%, a disease control rate (ORs + SD) of 80%, and median PFS of 52 weeks (32). Analysis of pretreatment plasma samples revealed that low (relative to median) plasma HGF levels correlated with increased tumor shrinkage (33). Cox regression analysis demonstrated a significant association between low baseline plasma HGF and increased PFS [low plasma HGF levels ($n = 108$), median PFS = 53 weeks; high plasma HGF levels ($n = 108$), median PFS = 28 weeks; $P = 0.016$; Supplementary Fig. S6]. These results indicate that HGF has a role of predictive biomarker of resistance to treatment with VEGFR TKIs in solid tumors other than NSCLC.

Discussion

Biologic agents targeting the VEGF pathway have produced significant clinical benefit in some cancers, including those that originate in the lung. However, therapeutic responses are usually short-lived, and resistance inevitably emerges. Several investigations concluded that both cancer cells and tumor-associated stromal cells can play critical roles in determining the sensitivity of a tumor to therapy (5, 13, 16, 21, 24). Nevertheless, elucidating the molecular mechanisms underlying NSCLC progression and its resistance to antiangiogenesis therapies has proved challenging. NSCLC is an extremely heterogeneous disease (37), and the fact that there are several classes of antiangiogenic therapies,

each possessing a different mechanism of action, adds to the complexity. Recently, we identified the mechanisms that mediate resistance of experimental NSCLC tumors to bevacizumab. However, less information is known regarding the mechanisms involved in the evolution of tumor resistance to therapies that bind to catalytic site of VEGFR. Here, we show that continued administration of the VEGFR TKIs cediranib and vandetanib to mice harboring established human lung cancers results in upregulation and activation of HGF/c-MET signaling networks in both the cancer cell and stromal cell compartments, which allows tumors to become refractory to therapy after an initial phase of response. Target cells for the stromal-derived HGF include the tumor-associated endothelial cells, which respond to the HGF signal by forming tortuous vascular networks. Combined inhibition of VEGFR and HGF receptor pathways prevents the vascular alterations and, moreover, delays the onset of therapeutic resistance in our models. In addition, our clinical analyses suggest that HGF is a predictive biomarker of VEGFR TKI resistance in that patients with cancer with low baseline plasma concentrations of HGF are more likely to benefit from VEGFR TKIs compared with patients with high HGF concentrations, who have a poorer PFS in multiple clinical trials.

We were able to identify stromal-derived HGF as a mediator of VEGFR TKI resistance by performing cross species–specific hybridization of microarrays on VEGFR TKI–treated tumors and comparing the patterns of gene expression of tumors that were sensitive to short-term VEGFR TKI treatment with tumors that were resistant to prolonged therapy. We elected to use 14 days as our time point for short-term treatment because H1975 tumors were responding to therapy at this time, but were still sufficiently large enough for analyses. Time-matched comparisons between resistant and responding tumors were prohibited because the sensitive tumors were too small to characterize and, in some cases, not detectable. In addition, the emergence of the resistant phenotype was sporadic and this prevented us from selecting one set time point for comparisons of resistant and sensitive tumors.

HGF is a plasminogen-like protein that mediates its effects by binding to the receptor tyrosine kinase encoded by the *MET* proto-oncogene (38, 39), referred to as c-MET, or hepatocyte growth factor receptor. c-MET is preferentially expressed in epithelial tissues and its phosphorylation activates transduction of a number of intracellular signaling pathways, including RAS/RAF, PI3K/AKT, and STAT3 (40, 41). Thus, phosphorylation of c-MET can activate programs that signal for cell survival, cell mobility, invasion, angiogenesis, epithelial-to-mesenchymal transition (EMT; ref. 42), and metastasis (43). HGF and c-MET are also localized at sites of pathological angiogenesis and are a potent endothelial mitogens (44–46). Indeed, we found that tumors treated with short-term VEGFR TKIs had reduced levels of c-MET compared with sensitive tumors, while c-MET was upregulated in tumors that progressed on long-term treatment. Ligand-induced activation of receptor tyrosine kinases (RTKs), including VEGFR1-3, PDGFR-β, RET and EGFR, has been shown to increase HIF-1α expression in neuroblastoma models, and pharmacologic inhibition of RTK activity can abrogate HIF-1α expression in cancer cells (47). We have shown that *EGFR*-mutant NSCLC cells, such as H1975 cells, express higher levels of c-MET and p-MET when compared with *EGFR* wild-type cells, and that EGFR inhibition in *EGFR*-mutant NSCLC models reduces c-MET expression and activation through a HIF-1α–dependent mechanism (48). We recently extended this finding to show that VEGFR TKIs, including vandetanib and cediranib, can modulate HIF-1α and c-MET in other subsets of NSCLC (49). Hence, there may be two opposing influences on c-MET levels via HIF-1α pathway: a short-term decrease in RTK-driven HIF-1α and c-MET levels in tumor cells, and a longer-term upregulation of c-MET, potentially in response to tumor hypoxia induced by the antiangiogenic effect of the drugs. This is consistent with our prior publications using the same NSCLC models and studies from others showing eventual induction of hypoxia after antiangiogenic therapy administered over time (50). c-MET is also enriched on dividing endothelial cells and is a marker of the angiogenic phenotype (46). The tumor vascular bed of H1975 tumors that were treated with short-term TKI therapy was reduced in comparison with vehicle-treated tumors, and this contributed, at least partially, to the reduction in total c-MET expression. As tumors are exposed to long-term RTK inhibition and acquire resistance, we observed an increase in tumor MVD and upregulation and activation of the HGF/c-MET axis, as compared with VEGFR TKI–sensitive tumors.

VEGF blockade has been shown to normalize the tumor vasculature by reducing interstitial pressure, thereby increasing perfusion, oxygenation, and drug delivery (51). However, there is some evidence that suggests these events are short-lived due to the excessive vessel pruning, which triggers hypoxia and prompts cancer cells to utilize alternative pathways for rapid tumor regrowth and rebound vascularization (52). Indeed, in other tumor models, antiangiogenic therapy was found to produce sustained hypoxia and impaired tumor vascular function, despite moderate vessel maturation (50). These findings support our observation that tumor hypoxia levels, as determined by CAIX staining on tumor tissues, increased in tumors that were sensitive to VEGFR TKIs compared with vehicle-treated tumors and remained elevated in the phase of acquired resistance to long-term antiangiogenic therapy. The tumor blood vessels supporting the cediranib- and vandetanib-resistant tumors were significantly more tortuous than vessels supplying tumors that were sensitive to TKI therapy. This finding is in contrast to our earlier report on NSCLC tumors that become resistant to bevacizumab following a prolonged period of antibody administration had a less tortuous vasculature (13). Indeed, we found that tumors that had acquired resistance to bevacizumab had a normalized tumor vasculature in that the tumor-associated blood vessels were covered in pericytes.

In addition to its effects on tumor and microvascular endothelial cells, HGF/c-MET signaling has also been implicated as central regulator of the drug-tolerant phenotype. In melanoma, HGF was found to play a role in mediating resistance to BRAF inhibition by activating MAPK and PI3K/AKT signaling through the c-MET receptor (53). In that cell-based study, stromal cells were the source of HGF secretion and resistance could be overcome by dual targeting of RAF and either HGF or c-MET. In a similar type of study, MET amplification was found to activate ERBB3/PI3K/AKT signaling in EGFR-mutant lung cancers and to enable the cancer cells to become resistance to EGFR TKIs (35). In another cell-based system, fibroblast-derived HGF was found to mediate EGFR TKI resistance in triple-negative breast cancer cells (54). Our observation that stromal HGF was upregulated in TKI-resistant tumors is in agreement with recent reports identifying the HGF/c-MET axis as an alternative mediator of resistance to sunitinib in preclinical tumor models (34). In our report, the strength of our technical approach using species-specific hybridization of microarrays on resistant and sensitive tumors lies in the ability to delineate whether the cancer cell or stromal cell compartment

(or both) is being modified by the therapeutic intervention. Dual VEGFR/c-MET pathway blockade delayed resistance compared with single signaling inhibition and reduced vessel sprouting. In animal models of spontaneous pancreatic neuroendocrine tumors, VEGF blockade promoted tumor invasion and metastasis, which could be inhibited by concurrent c-MET blockade (55). We acknowledge that as it is the case with other multityrosine kinase inhibitors, off-target effect of vandetanib and cediranib must be taken in consideration when interpreting the improved efficacy observed in our *in vivo* models with the combinations of VEGF/R inhibitors bevacizumab, cediranib, or vandetanib plus XL184. However, our contention that the HGF/c-MET pathway contributes to VEGF/R inhibitor resistance is supported by the use of the HGF-overexpressing models and our clinical findings. Our findings suggest that hypoxia-induced upregulation of the stromal HGF/c-MET axis may promote tumor growth and vascular changes observed in VEGFR TKI–resistant tumors through signaling activation in stromal cells. These observations reinforce the notion that the tumor-associated stroma plays an important, and in some cases dominant, role in NSCLC models of resistance to angiogenesis inhibitors.

Finally, we assessed the clinical relevance of our preclinical findings in patients with advanced/metastatic and refractory NSCLC treated with vandetanib, and patients with metastatic RCC treated with pazopanib. Prior studies suggest that broad plasma CAF profiling may be used to identify prognostic and predictive markers in patients with cancer (56–62). We measured serum levels in patients with advanced/metastatic and refractory NSCLC treated with vandetanib, and patients with metastatic RCC treated with the multi TKI pazopanib and identified a predictive role for circulating HGF as a marker of poor clinical benefit in mRCC and patients with NSCLC treated with VEGFR TKIs in three independent clinical trials (8, 12, 32, 33). Furthermore, our group has previously reported that high pretreatment levels of circulating HGF are associated with shorter PFS compared with placebo [32.1 weeks vs. 13.0 weeks; HR 0.46 (0.32–0.67) $P = 0.010$] in a phase III randomized study evaluating pazopanib in metastatic mRCC (63).

Our data suggest that patients with NSCLC with high circulating HGF levels may derive little benefit from the administration of VEGFR TKIs targeting the tumor microenvironment. These findings strengthen our preclinical results and lend credibility to our experimental approach for identifying mechanisms of resistance in NSCLC. Consistent with our preclinical observation, circulating HGF levels increase prior to disease progression in patients with colorectal cancer treated with the combination of chemotherapy and antiangiogenic therapy (64).

Taken together, our results indicate that HGF/c-MET signaling activation may represent a common mechanism of acquired resistance to VEGFR TKIs and may predict poor clinical outcome in patients treated with VEGFR inhibitors. As such, patients with high circulating HGF levels may derive poor relative benefit from VEGFR TKIs targeting the tumor microenvironment, in which both circulating host- and tumor-derived factors may affect therapeutic response. Dual VEGFR and HGF/c-MET targeting may represent a reasonable approach to improve patient outcomes.

Disclosure of Potential Conflicts of Interest

V. Haddad holds ownership interest (including patents) in AstraZeneca. J. Heymach is a consultant/advisory board member for AstraZeneca, EMD Serono, Genentech, Lilly, and Novartis. No potential conflicts of interest were disclosed by the other authors.

Authors' Contributions

Conception and design: T. Cascone, L. Xu, E.O. Hanrahan, J.M. Jüergensmeier, J. Heymach

Development of methodology: T. Cascone, L. Xu, H.T. Tran, J.-S. Lee, I.I. Wistuba, J. Heymach

Acquisition of data (provided animals, acquired and managed patients, provided facilities, etc.): T. Cascone, L. Xu, H.T. Tran, Y. Liu, E.O. Hanrahan, M.A. Cortez, U. Giri, B. Saigal, J. Wang, I.I. Wistuba, J. Heymach

Analysis and interpretation of data (e.g., statistical analysis, biostatistics, computational analysis): T. Cascone, L. Xu, H.Y. Lin, W. Liu, H.T. Tran, Y. Liu, K. Howells, M.A. Cortez, H. Kadara, Y.-Y. Park, W. Peng, J.-S. Lee, J.M. Juergensmeier, R.S. Herbst, J. Wang, I.I. Wistuba, J.J. Lee, J. Heymach

Writing, review, and/or revision of the manuscript: T. Cascone, L. Xu, H.Y. Lin, W. Liu, H.T. Tran, Y. Liu, E.O. Hanrahan, M. Nilsson, H. Kadara, W. Peng, A.J. Ryan, J.M. Juergensmeier, R.R. Langley, J.J. Lee, J. Heymach

Administrative, technical, or material support (i.e., reporting or organizing data, constructing databases): T. Cascone, L. Xu, V. Haddad, R.S. Herbst, R.R. Langley

Study supervision: J. Heymach

Acknowledgments

We gratefully acknowledge Donna Reynolds and Denise Wood for technical expertise, Emily B. Roarty, PhD, for expert assistance in the preparation of the manuscript, and Ericka Goodoff (University of Texas MD Anderson Cancer Center, Houston, TX) for the scientific editing of the manuscript.

Grant Support

This research was funded by The University of Texas Lung SPORE P50 CA070907, NIH Cancer Center Support Grant P30 CA016672, The University of Texas MD Anderson Cancer Center Head and Neck SPORE5 P50 CA097007, 1 R01 CA168484, the LUNGevity's Career Development Award for Translational Research, the Bruton Endowed Chair in Tumor Biology, and research support from AstraZeneca (all to J. Heymach).

The costs of publication of this article were defrayed in part by the payment of page charges. This article must therefore be hereby marked *advertisement* in accordance with 18 U.S.C. Section 1734 solely to indicate this fact.

Received December 21, 2016; revised April 19, 2017; accepted May 23, 2017; published OnlineFirst May 30, 2017.

References

1. Kerbel RS. Tumor angiogenesis. N Engl J Med 2008;358:2039–49.
2. Weis SM, Cheresh DA. Tumor angiogenesis: molecular pathways and therapeutic targets. Nat Med 2011;17:1359–70.
3. Carmeliet P, Jain RK. Molecular mechanisms and clinical applications of angiogenesis. Nature 2011;473:298–307.
4. Sandler A, Gray R, Perry MC, Brahmer J, Schiller JH, Dowlati A, et al. Paclitaxel-carboplatin alone or with bevacizumab for non-small-cell lung cancer. N Engl J Med 2006;355:2542–50.
5. Crawford Y, Ferrara N. Tumor and stromal pathways mediating refractoriness/resistance to anti-angiogenic therapies. Trends Pharmacol Sci 2009; 30:624–30.
6. Hurwitz H, Fehrenbacher L, Novotny W, Cartwright T, Hainsworth J, Heim W, et al. Bevacizumab plus irinotecan, fluorouracil, and leucovorin for metastatic colorectal cancer. N Engl J Med 2004;350: 2335–42.
7. Miller K, Wang M, Gralow J, Dickler M, Cobleigh M, Perez EA, et al. Paclitaxel plus bevacizumab versus paclitaxel alone for metastatic breast cancer. N Engl J Med 2007;357:2666–76.
8. Natale RB, Thongprasert S, Greco FA, Thomas M, Tsai CM, Sunpaweravong P, et al. Phase III trial of vandetanib compared with erlotinib in patients with previously treated advanced non-small-cell lung cancer. J Clin Oncol 2011;29:1059–66.

9. Lee JS, Hirsh V, Park K, Qin S, Blajman CR, Perng RP, et al. Vandetanib versus placebo in patients with advanced non-small-cell lung cancer after prior therapy with an epidermal growth factor receptor tyrosine kinase inhibitor: a randomized, double-blind phase III trial (ZEPHYR). J Clin Oncol 2012;30:1114–21.
10. Herbst RS, Sun Y, Eberhardt WE, Germonpre P, Saijo N, Zhou C, et al. Vandetanib plus docetaxel versus docetaxel as second-line treatment for patients with advanced non-small-cell lung cancer (ZODIAC): a double-blind, randomised, phase 3 trial. Lancet Oncol 2010;11:619–26.
11. de Boer RH, Arrieta O, Yang CH, Gottfried M, Chan V, Raats J, et al. Vandetanib plus pemetrexed for the second-line treatment of advanced non-small-cell lung cancer: a randomized, double-blind phase III trial. J Clin Oncol 2011;29:1067–74.
12. Heymach JV, Paz-Ares L, De Braud F, Sebastian M, Stewart DJ, Eberhardt WE, et al. Randomized phase II study of vandetanib alone or with paclitaxel and carboplatin as first-line treatment for advanced non-small-cell lung cancer. J Clin Oncol 2008;26:5407–15.
13. Cascone T, Herynk MH, Xu L, Du Z, Kadara H, Nilsson MB, et al. Upregulated stromal EGFR and vascular remodeling in mouse xenograft models of angiogenesis inhibitor-resistant human lung adenocarcinoma. J Clin Invest 2011;121:1313–28.
14. McIntyre A, Patiar S, Wigfield S, Li JL, Ledaki I, Turley H, et al. Carbonic anhydrase IX promotes tumor growth and necrosis in vivo and inhibition enhances anti-VEGF therapy. Clin Cancer Res 2012;18:3100–11.
15. Ebos JM, Kerbel RS. Antiangiogenic therapy: impact on invasion, disease progression, and metastasis. Nat Rev Clin Oncol 2011;8:210–21.
16. Shojaei F. Anti-angiogenesis therapy in cancer: Current challenges and future perspectives. Cancer Lett 2012;320:130–7.
17. Shojaei F, Wu X, Qu X, Kowanetz M, Yu L, Tan M, et al. G-CSF-initiated myeloid cell mobilization and angiogenesis mediate tumor refractoriness to anti-VEGF therapy in mouse models. Proc Natl Acad Sci U S A 2009;106:6742–7.
18. Shojaei F, Wu X, Malik AK, Zhong C, Baldwin ME, Schanz S, et al. Tumor refractoriness to anti-VEGF treatment is mediated by CD11b+Gr1+ myeloid cells. Nat Biotechnol 2007;25:911–20.
19. Ebos JM, Lee CR, Kerbel RS. Tumor and host-mediated pathways of resistance and disease progression in response to antiangiogenic therapy. Clin Cancer Res 2009;15:5020–5.
20. Casanovas O, Hicklin DJ, Bergers G, Hanahan D. Drug resistance by evasion of antiangiogenic targeting of VEGF signaling in late-stage pancreatic islet tumors. Cancer Cell 2005;8:299–309.
21. Chung AS, Wu X, Zhuang G, Ngu H, Kasman I, Zhang J, et al. An interleukin-17-mediated paracrine network promotes tumor resistance to anti-angiogenic therapy. Nat Med 2013;19:1114–23.
22. Shojaei F, Zhong C, Wu X, Yu L, Ferrara N. Role of myeloid cells in tumor angiogenesis and growth. Trends Cell Biol 2008;18:372–8.
23. Ebos JM, Lee CR, Cruz-Munoz W, Bjarnason GA, Christensen JG, Kerbel RS. Accelerated metastasis after short-term treatment with a potent inhibitor of tumor angiogenesis. Cancer Cell 2009;15:232–9.
24. Casanovas O. The adaptive stroma joining the antiangiogenic resistance front. J Clin Invest 2011;121:1244–7.
25. Wedge SR, Kendrew J, Hennequin LF, Valentine PJ, Barry ST, Brave SR, et al. AZD2171: a highly potent, orally bioavailable, vascular endothelial growth factor receptor-2 tyrosine kinase inhibitor for the treatment of cancer. Cancer Res 2005;65:4389–400.
26. Hennequin LF, Stokes ES, Thomas AP, Johnstone C, Ple PA, Ogilvie DJ, et al. Novel 4-anilinoquinazolines with C-7 basic side chains: design and structure activity relationship of a series of potent, orally active, VEGF receptor tyrosine kinase inhibitors. J Med Chem 2002;45:1300–12.
27. Wu W, Onn A, Isobe T, Itasaka S, Langley RR, Shitani T, et al. Targeted therapy of orthotopic human lung cancer by combined vascular endothelial growth factor and epidermal growth factor receptor signaling blockade. Mol Cancer Ther 2007;6:471–83.
28. Park ES, Kim SJ, Kim SW, Yoon SL, Leem SH, Kim SB, et al. Cross-species hybridization of microarrays for studying tumor transcriptome of brain metastasis. Proc Natl Acad Sci U S A 2011;108:17456–61.
29. Smyth GK. Limma: linear models for microarray data. Gentleman R, Dudoit S, Irizarry R, Huber W, editors. New York, NY: Springer; 2005.
30. Pounds S, Morris SW. Estimating the occurrence of false positives and false negatives in microarray studies by approximating and partitioning the empirical distribution of p-values. Bioinformatics 2003;19:1236–42.
31. Van den Eynden GG, Van Laere SJ, Van der Auwera I, Gilles L, Burn JL, Colpaert C, et al. Differential expression of hypoxia and (lymph)angiogenesis-related genes at different metastatic sites in breast cancer. Clin Exp Metastasis 2007;24:13–23.
32. Hutson TE, Davis ID, Machiels JP, De Souza PL, Rottey S, Hong BF, et al. Efficacy and safety of pazopanib in patients with metastatic renal cell carcinoma. J Clin Oncol 2010;28:475–80.
33. Tran HT, Liu Y, Zurita AJ, Lin Y, Baker-Neblett KL, Martin AM, et al. Prognostic or predictive plasma cytokines and angiogenic factors for patients treated with pazopanib for metastatic renal-cell cancer: a retrospective analysis of phase 2 and phase 3 trials. Lancet Oncol 2012;13:827–37.
34. Shojaei F, Lee JH, Simmons BH, Wong A, Esparza CO, Plumlee PA, et al. HGF/c-Met acts as an alternative angiogenic pathway in sunitinib-resistant tumors. Cancer Res 2010;70:10090–100.
35. Turke AB, Zejnullahu K, Wu YL, Song Y, Dias-Santagata D, Lifshits E, et al. Preexistence and clonal selection of MET amplification in EGFR mutant NSCLC. Cancer Cell 2010;17:77–88.
36. Timar J, Dome B. Antiangiogenic drugs and tyrosine kinases. Anticancer Agents Med Chem 2008;8:462–9.
37. Zhang J, Fujimoto J, Zhang J, Wedge DC, Song X, Zhang J, et al. Intratumor heterogeneity in localized lung adenocarcinomas delineated by multiregion sequencing. Science 2014;346:256–9. doi: 10.1126/science.1256930.
38. Bottaro DP, Rubin JS, Faletto DL, Chan AM, Kmiecik TE, Vande Woude GF, et al. Identification of the hepatocyte growth factor receptor as the c-met proto-oncogene product. Science 1991;251:802–4.
39. Naldini L, Vigna E, Narsimhan RP, Gaudino G, Zarnegar R, Michalopoulos GK, et al. Hepatocyte growth factor (HGF) stimulates the tyrosine kinase activity of the receptor encoded by the proto-oncogene c-MET. Oncogene 1991;6:501–4.
40. Galimi F, Brizzi MF, Comoglio PM. The hepatocyte growth factor and its receptor. Stem Cells 1993;11 Suppl 2:22–30.
41. Hecht M, Papoutsi M, Tran HD, Wilting J, Schweigerer L. Hepatocyte growth factor/c-Met signaling promotes the progression of experimental human neuroblastomas. Cancer Res 2004;64:6109–18.
42. Birchmeier C, Birchmeier W, Gherardi E, Vande Woude GF. Met, metastasis, motility and more. Nat Rev Mol Cell Biol 2003;4:915–25.
43. Gherardi E, Birchmeier W, Birchmeier C, Vande Woude G. Targeting MET in cancer: rationale and progress. Nat Rev Cancer 2012;12:89–103.
44. Rosen EM, Grant DS, Kleinman HK, Goldberg ID, Bhargava MM, Nickoloff BJ, et al. Scatter factor (hepatocyte growth factor) is a potent angiogenesis factor in vivo. Symp Soc Exp Biol 1993;47:227–34.
45. Bussolino F, Di Renzo MF, Ziche M, Bocchietto E, Olivero M, Naldini L, et al. Hepatocyte growth factor is a potent angiogenic factor which stimulates endothelial cell motility and growth. J Cell Biol 1992;119:629–41.
46. Ding S, Merkulova-Rainon T, Han ZC, Tobelem G. HGF receptor upregulation contributes to the angiogenic phenotype of human endothelial cells and promotes angiogenesis in vitro. Blood 2003;101:4816–22.
47. Nilsson MB, Zage PE, Zeng L, Xu L, Cascone T, Wu HK, et al. Multiple receptor tyrosine kinases regulate HIF-1alpha and HIF-2alpha in normoxia and hypoxia in neuroblastoma: implications for antiangiogenic mechanisms of multikinase inhibitors. Oncogene 2010;29:2938–49.
48. Xu L, Nilsson MB, Saintigny P, Cascone T, Herynk MH, Du Z, et al. Epidermal growth factor receptor regulates MET levels and invasiveness through hypoxia-inducible factor-1alpha in non-small cell lung cancer cells. Oncogene 2010;29:2616–27.
49. Nilsson MB, Giri U, Gudikote J, Tang X, Lu W, Tran H, et al. KDR amplification is associated with VEGF-induced activation of the mTOR and invasion pathways but does not predict clinical benefit to the VEGFR TKI vandetanib. Clin Cancer Res 2016;22:1940–50.
50. Franco M, Man S, Chen L, Emmenegger U, Shaked Y, Cheung AM, et al. Targeted anti-vascular endothelial growth factor receptor-2 therapy leads to short-term and long-term impairment of vascular function and increase in tumor hypoxia. Cancer Res 2006;66:3639–48.
51. Jain RK. Normalizing tumor vasculature with anti-angiogenic therapy: a new paradigm for combination therapy. Nat Med 2001;7:987–9.

52. Carmeliet P, Jain RK. Principles and mechanisms of vessel normalization for cancer and other angiogenic diseases. Nat Rev Drug Discov 2011;10:417–27.
53. Straussman R, Morikawa T, Shee K, Barzily-Rokni M, Qian ZR, Du J, et al. Tumour micro-environment elicits innate resistance to RAF inhibitors through HGF secretion. Nature 2012;487:500–4.
54. Mueller KL, Madden JM, Zoratti GL, Kuperwasser C, List K, Boerner JL. Fibroblast-secreted hepatocyte growth factor mediates epidermal growth factor receptor tyrosine kinase inhibitor resistance in triple-negative breast cancers through paracrine activation of Met. Breast Cancer Res 2012;14:R104.
55. Sennino B, Ishiguro-Oonuma T, Wei Y, Naylor RM, Williamson CW, Bhagwandin V, et al. Suppression of tumor invasion and metastasis by concurrent inhibition of c-Met and VEGF signaling in pancreatic neuroendocrine tumors. Cancer Discov 2012;2:270–87.
56. Nikolinakos PG, Altorki N, Yankelevitz D, Tran HT, Yan S, Rajagopalan D, et al. Plasma cytokine and angiogenic factor profiling identifies markers associated with tumor shrinkage in early-stage non-small cell lung cancer patients treated with pazopanib. Cancer Res 2010;70:2171–9.
57. Hanrahan EO, Lin HY, Kim ES, Yan S, Du DZ, McKee KS, et al. Distinct patterns of cytokine and angiogenic factor modulation and markers of benefit for vandetanib and/or chemotherapy in patients with non-small-cell lung cancer. J Clin Oncol 2010;28:193–201.
58. Hanrahan EO, Ryan AJ, Mann H, Kennedy SJ, Langmuir P, Natale RB, et al. Baseline vascular endothelial growth factor concentration as a potential predictive marker of benefit from vandetanib in non-small cell lung cancer. Clin Cancer Res 2009;15:3600–9.
59. Montero AJ, Diaz-Montero CM, Millikan RE, Liu J, Do KA, Hodges S, et al. Cytokines and angiogenic factors in patients with metastatic renal cell carcinoma treated with interferon-alpha: association of pretreatment serum levels with survival. Ann Oncol 2009;20:1682–7.
60. Pena C, Lathia C, Shan M, Escudier B, Bukowski RM. Biomarkers predicting outcome in patients with advanced renal cell carcinoma: results from sorafenib phase III Treatment Approaches in Renal Cancer Global Evaluation Trial. Clin Cancer Res 2010;16:4853–63.
61. Zurita AJ, Jonasch E, Wang X, Khajavi M, Yan S, Du DZ, et al. A cytokine and angiogenic factor (CAF) analysis in plasma for selection of sorafenib therapy in patients with metastatic renal cell carcinoma. Ann Oncol 2012;23:46–52.
62. Heymach JV, Jonasch E, Wang X, Du DZ, Yan S, Xu L, et al. A cytokine and angiogenic factor (CAF) plasma signature for selection of sorafenib (SR) therapy in patients (pts) with metastatic renal cell carcinoma (mRCC). J Clin Oncol 2009 27 (suppl):15S (abstr 5114).
63. Sternberg CN, Davis ID, Mardiak J, Szczylik C, Lee E, Wagstaff J, et al. Pazopanib in locally advanced or metastatic renal cell carcinoma: results of a randomized phase III trial. J Clin Oncol 2010;28:1061–8.
64. Kopetz S, Hoff PM, Morris JS, Wolff RA, Eng C, Glover KY, et al. Phase II trial of infusional fluorouracil, irinotecan, and bevacizumab for metastatic colorectal cancer: efficacy and circulating angiogenic biomarkers associated with therapeutic resistance. J Clin Oncol 2010;28:453–9.